Journal of Applied Polymer Science

Wetting behavior of polymer melts on coated and uncoated tool steel surfaces

Gernot Zitzenbacher,[1] Zefeng Huang,[1] Manuel Längauer,[1] Christian Forsich,[1] Clemens Holzer[2]

[1]Department of Materials Technology School of Engineering and Environmental Sciences, University of Applied Sciences Upper Austria, Stelzhamerstr. 23, 4600, Wels, Austria

[2]Department Polymer Engineering and Science, Chair of Polymer Processing, Otto Gloeckel-Straße 2, Leoben, 8700, Austria, Montanuniversitaet Leoben

Correspondence to: G. Zitzenbacher (E-mail: g.zitzenbacher@fh-wels.at)

ABSTRACT: The wettability of steel and coatings used for tools and screws in polymer processing is often determined at room temperature. However, it has to be taken into account that polymeric materials are processed at higher temperatures. Contact angle measurements of melted PP, HDPE, PMMA, and PA 6.6 on steel and on TiN, TiAlN, CrN, DLC, and PTFE were performed in this work to investigate the wetting behavior under closer-to-processing conditions. The contact angle is dependent on time and the ambient atmosphere. Oxidation and degradation of the polymer melts influence wetting significantly. TiN, TiAlN, CrN, and DLC exhibit a rather good wettability, whereas the highest contact angle of the polymer melts was observed with PTFE. Higher roughnesses of the surfaces lead to an increase in the contact angle. It was also shown that a higher temperature causes a better wetting of the solid surfaces. © 2016 Wiley Periodicals, Inc. J. Appl. Polym. Sci. **2016**, *133*, 43469.

KEYWORDS: extrusion; molding; polyamides; polyolefins; surfaces and interfaces

Received 16 October 2015; accepted 23 January 2016
DOI: 10.1002/app.43469

INTRODUCTION

Coatings which are deposited by physical vapor deposition (PVD) or by chemical vapor deposition (CVD) on tool or screw surfaces, such as titanium nitride (TiN) and diamond-like carbon (DLC), are used in polymer processing because they increase the wear resistance, prevent material debris and degradation, and also improve product quality.[1,2] The wetting behavior and surface energy of such materials is usually measured at room temperature using liquids of known surface tension.[3,4] However, it must be taken into account that in polymer processing, polymeric materials are processed at a higher temperature. Furthermore, different problems arise in these processes which require a better understanding of data about the wetting of polymer melts on tool and mold surfaces at process-related temperatures. For example, wall sliding of the polymer melt flow, instabilities such as shark skin and the extrusion pressure can be influenced by the tool material.[5–9]

The wetting of melted polymeric materials is different to data evaluated at room temperature. Few studies are available on this issue in the literature. Anastasiadis *et al.* investigated the wetting of linear low density and high density polyethylene on steel and fluoropolymer coatings.[10] Kopczynska *et al.* determined the surface tension of melted polycarbonate (PC), polystyrene (PS), styrene acrylonitrile (SAN), polyethylene (PE), and polyamide 6 (PA 6).[11,12] Yang *et al.* also measured the contact angle of PS and PMMA on a Si and a Ni substrate.[12]

Contact angle measurements of polymer melts on tool steel samples with different surface treatment and coatings were performed in this paper to get a better understanding of the wetting behavior under closer-to-processing conditions. The polymeric materials used are polypropylene (PP), high density polyethylene (HDPE), polymethylmethacrylate (PMMA), and polyamide 6.6 (PA 6.6). The metal samples are steels with different surface roughnesses, as well as steel coated with titanium aluminum nitride (TiAlN), titanium nitride (TiN), chromium nitride (CrN), Si-doped diamond-like carbon (DLC) and polytetrafluoroethylene (PTFE). During the experiments, the polymeric material was placed on the hot solid sample in a high temperature chamber. The time-dependent drop shape was recorded using a CCD camera system and the contact angle was evaluated from these data. The measuring temperature was chosen according to common processing conditions.

The results show that the wettability of these PVD and CVD coatings with the polymer melts is similar to steel. It was observed that a roughening of the steel surface can influence the contact angle more than the PVD and CVD coatings used.

© 2016 Wiley Periodicals, Inc.

Ideally, the surface should exhibit a relatively high roughness and a low surface energy to provide a higher contact angle of the polymer melt. It was also found that the wettability depends on the surface tension of the polymer melt. The influence of temperature, residence time and the ambient atmosphere on the measured contact angle is significantly higher than the properties of the solid surfaces.

THEORETICAL BACKGROUND

Some basic models describe the wetting of solid surfaces by liquids. First of all, Young's equation is fundamental for wetting. It is assumed that a sessile drop contacts an ideally rigid, homogeneous, flat, and inert surface. The contact area between the drop and the substrate is a disk. There is a circular contact line around this disk, and the joining angle of the liquid to the solid is the contact angle θ. Then the surface energy between the solid and the liquid σ_{SL} can be described by eq. (1), where σ_S is the surface energy of the solid and σ_L is the surface tension of the liquid[13]

$$\sigma_{SL}=\sigma_S-\sigma_L\cdot\cos\theta. \quad (1)$$

It has to be considered that real surfaces are not ideally smooth and exhibit a certain surface roughness. Wenzel proposed eq. (2), which relates the contact angle to surface roughness and surface energy, where $\theta_W{}^*$ is the apparent contact angle influenced by the roughness of the solid surface, and r is the roughness factor[14]

$$r\cdot(\sigma_S-\sigma_{SL})=\sigma_L\cdot\cos\theta_W^*. \quad (2)$$

The roughness factor is also described as the roughness area ratio of the actual surface with respect to the geometric surface. With eq. (1) the Wenzel equation can be rewritten to

$$r\cdot\cos\theta=\cos\theta_W{}^*, \quad (3)$$

where θ is the real contact angle of an ideally smooth surface. According to Blossey, the Wenzel equation predicts that a higher surface roughness can improve the wettability of a hydrophilic surface, yet may decrease that of a hydrophobic substrate.[15]

The Wenzel equation assumes homogenous wetting, which means that the liquid penetrates the cavities of the solid's surface structure and contacts the whole surface. When heterogenous wetting occurs, only the tops of the protrusions of the solid's surface are contacted by the liquid as air bubbles are trapped inside the surface structure below the liquid. Heterogenous wetting can be described by the Cassie–Baxter equation. It is assumed that if there were only air between the solid and the liquid, the contact angle would be 180 °. Then the contact angle θ is[16,17]

$$\cos\theta^*=-1+f\cdot(\cos\theta+1)=f\cdot\cos\theta+f-1, \quad (4)$$

where θ^* is the apparent contact angle influenced by the roughness of the solid surface and f is the ratio of the total area of the solid–liquid interface with respect to the total area of solid–liquid and liquid–air interfaces in a plane geometrical area of unity parallel to the rough surface. When the ratio r_f of the actual wetted area to the projected area is introduced in eq. (4), it results in a modified form of the Cassie-Baxter equation[17]

$$\cos\theta_{CB}{}^*=r_f f\cdot\cos\theta+f-1, \quad (5)$$

where $\theta_{CB}{}^*$ is the apparent contact angle influenced by the roughness of the solid surface.

The surface energy of solids can be determined using test liquids with known surface tension. Owens proposed a model to evaluate the dispersive $\sigma_{s,dis}$ and the polar fraction $\sigma_{s,pol}$ of surface energy of the solid surface[18]

$$\frac{1+\cos\theta}{2}\cdot\frac{\sigma_L}{\sqrt{\sigma_{L,dis}}}=\sqrt{\sigma_{s,pol}}\cdot\sqrt{\frac{\sigma_{L,pol}}{\sigma_{L,dis}}}+\sqrt{\sigma_{s,dis}}, \quad (6)$$

where θ is the contact angle, $\sigma_{L,dis}$ is the dispersive fraction of the surface energy of the liquid, $\sigma_{L,pol}$ is the polar fraction of surface energy of the liquid and σ_L is the total surface energy of the liquid.

EXPERIMENTAL

Materials

The experiments were conducted with four different polymers. The two polyolefins were a high density polyethylene (HDPE) MG 9641 and a polypropylene homopolymer (PP) HD 120 MO, both produced by Borealis, Linz, Austria, which are usually used for injection molding applications. HDPE MG 9641 has a melt flow rate (MFR) of 8 g (10 min)$^{-1}$ at (190 °C/2.16 kg) and PP HD 120 MO has a MFR of 8 g (10 min)$^{-1}$ at (230 °C/2.16 kg). The polymethylmethacrylate (PMMA) PLEXIGLAS 7*M* from EVONIK, Darmstadt, Germany is suitable for extruded profiles and panels in lighting engineering and has a MFR of 3.45 g (10 min)$^{-1}$ at (230 °C/3.80 kg). Polyamide 6.6 (PA 6.6) Durethan 30 S from LANXESS, Cologne, Germany is an injection molding grade with a MFR of 75 g (10 min)$^{-1}$ at (270 °C/5.00 kg). The reported MFR values were provided by the material suppliers.

Solid discs with a diameter of 40 mm and a thickness of 10 mm were used as substrates to evaluate the wetting of the melted polymeric materials. Polished and ground steel X38CrMoV5-1 as well as TiN, TiAlN, CrN, PTFE, and Si-doped amorphous DLC-coated steel samples were used for the experiments. The two DLC coatings, which were used, exhibit a different Si concentration, DLC A 28 at% and DLC B 13 at%, respectively.

Prior to coating, a heat treatment of the samples was performed to achieve a sufficiently high surface hardness on which to deposit the coatings. Then, all steel inserts except the ground steel were polished to a surface roughness S_a of ~27 nm. TiN, TiAlN, and CrN were deposited using a PVD process. The DLC coatings were produced in a PACVD process (plasma assisted chemical vapor deposition). After roughening of the metal surface and treatment with a primer, the PTFE coating was deposited in a sintering process.

Determination of Surface Roughness

The surface roughness of the solid disc samples was determined by means of a confocal microscope DCM3D, Leica Microsystems, Wetzlar, Germany. Scans were carried out to measure the surface topology at three positions located 8.7 mm from the center of the disc. The rectangular measuring window around

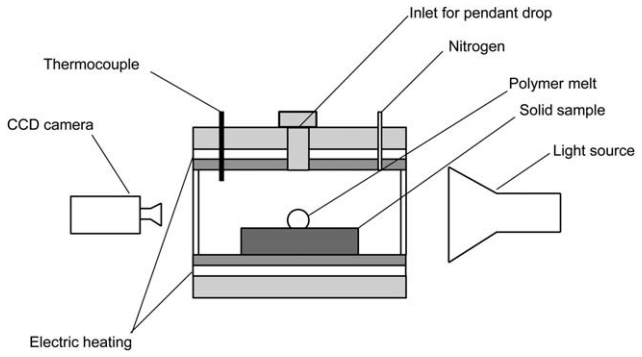

Figure 1. Experimental setup for the determination of the contact angle (schematic drawing).

each position had the dimensions 1.63 mm × 1.74 mm. The selected magnification factor was 50. With this data, an area weighted surface roughness S_a was evaluated using the software Leica Map.

Determination of Surface Energy of the Solid Samples

The surface energy of the solid disc samples was determined at room temperature using a contact angle measurement system DSA 30 S, Kruess, Hamburg, Germany. The contact angles of the measuring liquids were detected employing the sessile drop method. The dosing rate was 50 µL min^{-1} and the drop volume was 10 µL. The tests were carried out three times for each pairing of measuring liquid and solid substrate. Then the dispersive $\sigma_{s,dis}$ and the polar fraction $\sigma_{s,pol}$ of surface energy were evaluated according to Owens *et al.*[18] The measuring liquids used were deionized water (polar, $\sigma_L = 72.8$ mN m^{-1}, $\sigma_{L,dis} = 21.8$ mN m^{-1}, $\sigma_{L,pol} = 51.0$ mN m^{-1}), diiodmethane (nonpolar, $\sigma_L = 50.8$ mN m^{-1}, $\sigma_{L,dis} = 50.8$ mN m^{-1}, $\sigma_{L,pol} = 0$ mN m^{-1}) and 1,5-pentanediol (partially polar, $\sigma_L = 43.3$ mN m^{-1}, $\sigma_{L,dis} = 27.6$ mN m^{-1}, $\sigma_{L,pol} = 15.7$ mN m^{-1}) to determine the polar and dispersive fraction of surface energy of the solid substrates in this study. The values of surface energy for the measuring liquids were taken from the database of the analysis software from the contact angle measurement system.

Determination of the Contact Angle of the Polymer Melts

A Kruess Drop Shape Analyzer DSA 30S with a high temperature sample chamber TC 21 was used in the course of this research to measure the contact angle of the melted polymeric materials on the solid surfaces (see Figure 1). The temperature of the measuring chamber was adjusted by a control system. The measuring process was carried out under inert gas atmosphere (nitrogen gas) to prevent the oxidative degradation of the polymer melt and the oxidation of the metal substrates. The nitrogen gas used was Alphagaz™, Air Liquide Austria, Schwechat, Austria with a pureness of over 99.999%. The gas flow rate was 20 Nl h^{-1}, which means that the gas volume of the high temperature chamber was changed every 45 s. The analysis was then carried out with corresponding software.

The surface of the solid sample was cleaned carefully with isopropanol in the first step of the test using a tissue and dried with an air stream. Then the solid sample was placed in the high temperature chamber. After preheating the measuring chamber for 15 min, the polymeric granule was placed on the solid surface with a pair of tweezers. This step had to be done as fast as possible to avoid a higher temperature drop and nitrogen loss in the measuring chamber. The melt drop was formed and the drop shape was recorded dependent on time with a CCD camera with a rate of 1 fps. The total recording time was ~30 min, but the first 5 min were not considered in the evaluation due to melting of the polymeric sample. Then the contact angle was determined dependent on time using the video data. In the evaluation the drop contour was approximated with a polynomial function near the base line. The incline of the approximation function in the contact point of the three phases was used to evaluate the contact angle. Each test was carried out three times in order to verify its reproducibility and a mean value was calculated. The testing temperature of the polymeric materials was chosen according to common processing conditions.

RESULTS

Surface Roughness and Surface Energy of the Solid Samples

The surface properties of the solid substrates including their standard deviations are summarized in Table I. The surface energy values of the solid samples including the polar and dispersive fraction are also shown graphically in Figure 2. The low standard deviation values indicate the good reproducibility of the tests. It was observed that DLC A exhibits the lowest surface

Table I. Surface Roughness S_a, Surface Energy σ_S, Dispersive Fraction of Surface Energy $\sigma_{s,dis}$, and Polar Fraction of Surface Energy $\sigma_{s,polar}$ of the Solid Samples Including Their Standard Deviations (s_{Sa}, s_σ, $s_{\sigma s,dis}$, $s_{\sigma s,polar}$)

Surface	S_a (nm)	s_{Sa} (nm)	σ_S (mN m^{-1})	s_σ (mN m^{-1})	$\sigma_{s,dis}$ (mN m^{-1})	$s_{\sigma s,dis}$ (mN m^{-1})	$\sigma_{s,polar}$ (mN m^{-1})	$s_{\sigma s,polar}$ (mN m^{-1})
Polished steel	31.3	3.9	33.5	0.9	29.2	0.7	4.3	0.5
Ground steel	76.1	7.0	35.8	1.2	28.5	0.8	7.2	0.9
PTFE	958.7	41.3	19.6	0.8	17.8	0.7	1.7	0.3
TiAlN	30.0	2.6	40.0	0.5	26.4	0.4	13.5	0.3
TiN	63.5	6.6	42.1	0.2	27.3	0.1	14.8	0.2
CrN	35.4	4.5	36.3	0.6	30.6	0.5	5.7	0.4
DLC A	24.7	2.2	40.2	0.9	29.3	0.8	10.8	0.5
DLC B	33.3	1.5	38.9	0.9	29.6	0.4	9.3	0.8

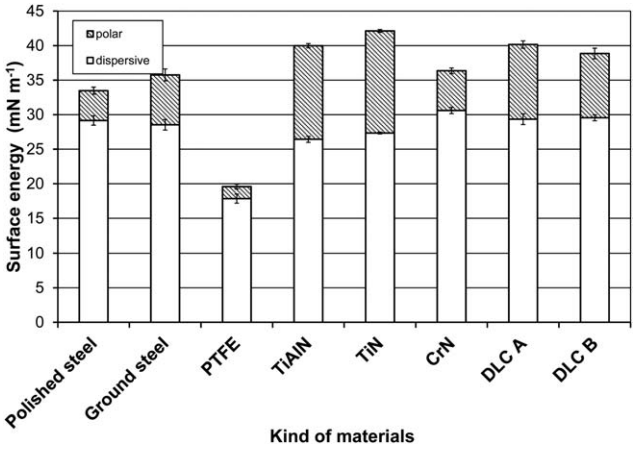

Figure 2. Total surface energy, polar fraction, and dispersive fraction of surface energy of the solid samples.

roughness ($S_a = 24.7$ nm). TiAlN ($S_a = 30.0$ nm), polished steel ($S_a = 31.3$ nm), DLC B ($S_a = 33.3$ nm) and CrN ($S_a = 35.4$ nm) are similarly rough. TiN ($S_a = 63.5$ nm), and ground steel ($S_a = 76.1$ nm) are rougher, but the PTFE coating has the highest roughness ($S_a = 958.7$ nm).

PTFE exhibits the lowest surface energy ($\sigma_S = 19.6$ mN m^{-1}) and TiN ($\sigma_S = 42.1$ mN m^{-1}) the highest. DLC A ($\sigma_S = 40.2$ mN m^{-1}), TiAlN ($\sigma_S = 40.0$ mN m^{-1}) and DLC B ($\sigma_S = 38.9$ mN m^{-1}) have a similarly high surface energy. CrN ($\sigma_S = 36.3$ mN m^{-1}) exhibits the lowest surface energy of the PVD and CVD coatings studied. The surface energy of polished steel is 33.5 mN m^{-1}. The steel surface with a higher roughness also exhibits a similar surface energy.

When the solid substrates are listed regarding to increasing polarity, PTFE has a low polar surface ($\sigma_{s,polar} = 1.7$ mN m^{-1}), followed by CrN which shows the lowest polarity ($\sigma_{s,polar} = 5.7$ mN m^{-1}) of the PVD and CVD coatings used. DLC A ($\sigma_{s,polar} = 10.8$ mN m^{-1}) and DLC B ($\sigma_{s,polar} = 9.3$ mN m^{-1}) have higher polarity. TiAlN ($\sigma_{s,polar} = 13.5$ mN m^{-1}) and TiN ($\sigma_{s,polar} = 14.8$ mN m^{-1}) have the highest polarities. Polished steel ($\sigma_{s,polar} = 4.3$ mN m^{-1}) has a similar polarity to CrN.

Influence of the Ambient Atmosphere on the Contact Angle

Oxygen in the ambient atmosphere can cause oxidation of the polymeric material at higher temperatures. The wetting behavior of the polymer melt on the solid surface can be influenced in this way. First of all, experiments in air and nitrogen were conducted to point out the influence of the atmosphere in the high temperature chamber on the measured contact angle. These tests were performed with polypropylene, because it is sensitive to oxidation.[19] Polypropylene was melted on polished steel at a temperature of 200 °C. Figure 3 shows the evaluated contact angle θ dependent on time t in air and nitrogen, Figure 4 shows pictures of the recorded drop shape after 0 s, 400 s, 800 s, 1200 s and 1600 s. It can be observed that the contact angle decreases with time. Using nitrogen, the mean value of the contact angle of the polypropylene melt is 131.4 ° at the beginning (t = 0 s) and decreases continuously. No stable state can be reached and the contact angle is 77.1° at the end of the measuring runs

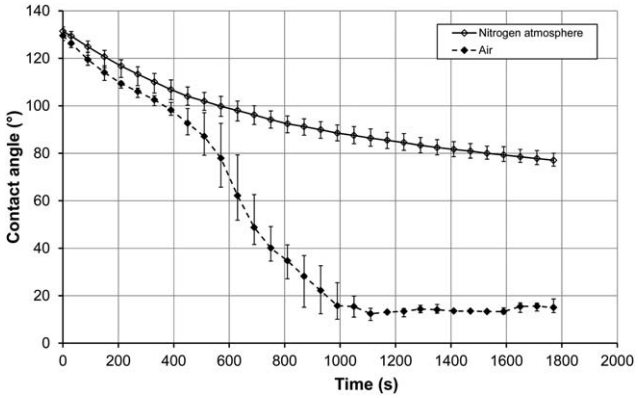

Figure 3. Contact angle of the polypropylene melt on polished steel dependent on time at a temperature of 200 °C in nitrogen and in air.

(t = 1770 s). In air, the contact angle of polypropylene is very similar to the measured value in nitrogen ($\theta = 129.6°$) at the beginning (t = 0 s). The decrease in the contact angle with time is larger compared to that in the nitrogen atmosphere. After a measuring time of approximately 400 s a steep decrease in the contact angle occurs. Later, the polypropylene melt drop reaches a stable state after approximately 1100 s. At the end of the measuring run the contact angle is 15.0°. There is a completely different wetting behavior when using nitrogen or air. Wetting of the polymer melt on the steel sample in air is significantly better than in nitrogen. As a consequence of these tests, all the following experiments were carried out in nitrogen to minimize material oxidation.

Influence of Temperature on the Contact Angle

The influence of temperature on the wetting of polypropylene on polished steel is shown in Figure 5. Better wetting can be observed at higher temperatures. At the beginning (t = 0 s), the contact angle of polypropylene is 135.4°, 131.4° and 119.4° at a temperature of 185 °C, 200 °C and 210 °C. At the end of the measuring runs (t = 1770 s) there is a decrease in the contact angle to the values 85.0°, 77.1° and 72.6° at a temperature of 185 °C, 200 °C and 210 °C, respectively.

Influence of Surface Roughness on the Contact Angle

The effect of surface roughness S_a is demonstrated using polished ($S_a = 31.3$ nm) and ground steel ($S_a = 76.1$ nm) as a solid substrate. Figure 6 shows the contact angle of high density polyethylene and polypropylene dependent on time at a temperature of 210 °C. Both polymeric materials exhibit a decrease in the contact angle with time. A stable contact angle of high density polyethylene is reached after approximately 1200 s, but polypropylene shows no stable contact angle. An increase in the contact

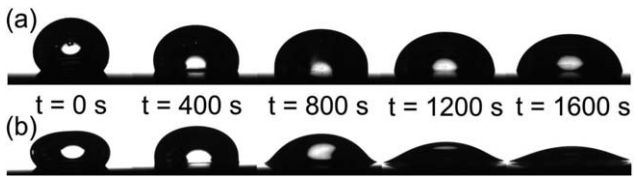

Figure 4. Drop shape of the polypropylene melt on polished steel at a temperature of 200 °C in nitrogen (a) and air (b) after different measuring times.

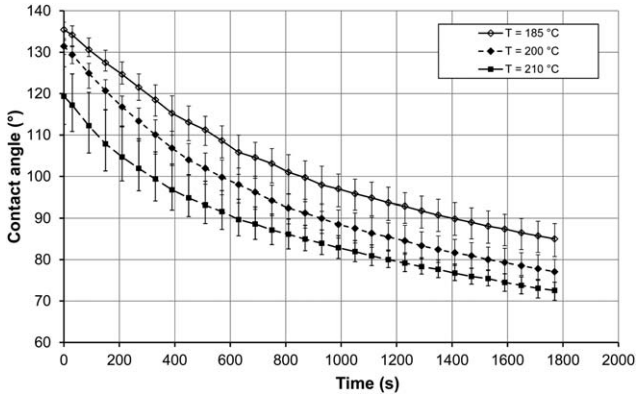

Figure 5. Contact angle of the polypropylene melt on polished steel dependent on time at the temperatures 185, 200, and 210 °C.

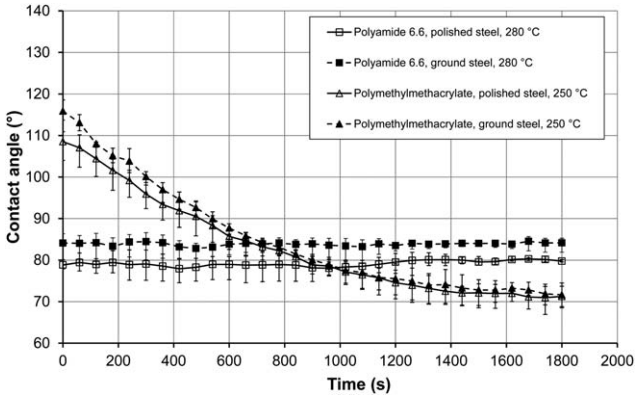

Figure 7. Contact angle of the polyamide 6.6 and the polymethylmethacrylate melt dependent on time on different rough steel surfaces.

angle of polypropylene can be observed with a higher roughness. High density polyethylene reveals a completely different behavior. There is a decrease in the contact angle with higher surface roughness.

At the beginning (t = 0 s), the high density polyethylene melt forms a contact angle of 106° on polished steel and 97° on ground steel. At the end of the measurement run the contact angle is 71.2° on polished steel and 65.1° on ground steel.

Polypropylene has a higher contact angle than high density polyethylene at the beginning (t = 0 s). The contact angle is 119.4° on polished steel and 124.5° on ground steel. It can be seen that with a longer measuring time a decrease in the contact angle occurs. In the end, there is no difference between the two surfaces (polished steel: $\theta = 72.6°$, ground steel: $\theta = 74.1°$). Furthermore, the contact angle is very similar to high density polyethylene on polished steel.

The contact angle of polyamide 6.6 and polymethylmethacrylate on polished and ground steel dependent on time is depicted in Figure 7. Polyamide 6.6 was tested at a temperature of 280 °C and polymethylmethacrylate at 250 °C. Polyamide 6.6 has a rather constant contact angle. Polymethylmethacrylate exhibits a decrease in the contact angle with time, but a stable state can be reached after approximately 1400 s. Polyamide 6.6 reveals an increase in the contact angle with a higher surface roughness.

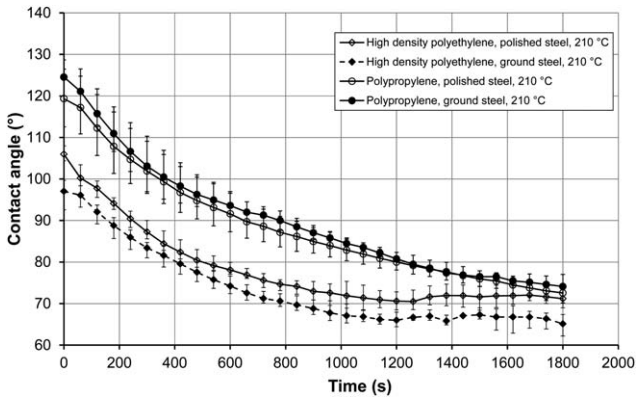

Figure 6. Contact angle of the polypropylene and the high density polyethylene melt dependent on time on different rough steel surfaces.

At the beginning (t = 0 s), the contact angle of polyamide 6.6 is 78.8° on polished steel and 84.1° on ground steel. At the end, the contact angle is 79.8° on polished steel and 84.1° on ground steel. Polymethylmethacrylate exhibits a clear influence of surface roughness on the wetting at the beginning (t = 0 s), where the contact angle is 108.5° on polished steel and 115.9° on ground steel. The difference between the contact angle values measured on different rough steel surfaces vanishes by the end of the test run, where the contact angle of polymethylmethacrylate is 71.3° on polished steel and 71.6° on ground steel.

Influence of the Different Solid Surfaces on the Contact Angle

The effect of the different solid surfaces used on the wetting of the polymer melts is represented in histograms showing the contact angle at the start and the end of the test runs. The contact angle values of high density polyethylene at a temperature of 210 °C, of polypropylene at a temperature of 200 °C, of polyamide 6.6 at a temperature of 280 °C and of polymethylmethacrylate at a temperature of 250 °C are depicted in Figures 8–11.

At the start of the test procedure (t = 0 s) the highest contact angle of the high density polyethylene melt can be observed on polished steel ($\theta = 106°$), and the lowest value occurs on CrN

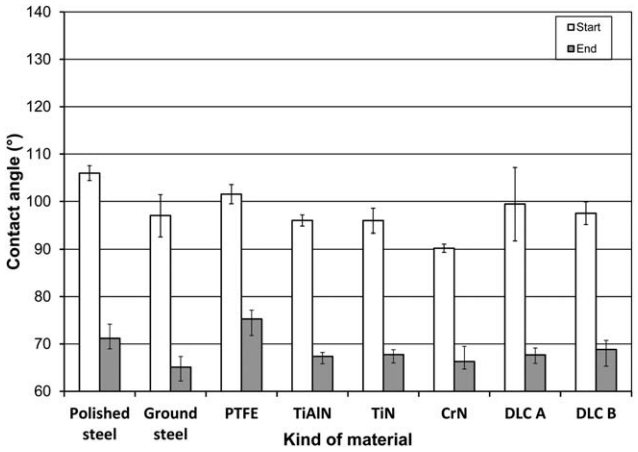

Figure 8. Contact angle of the high density polyethylene melt on the different surfaces at a temperature of 210 °C at the start and the end of the measuring procedure.

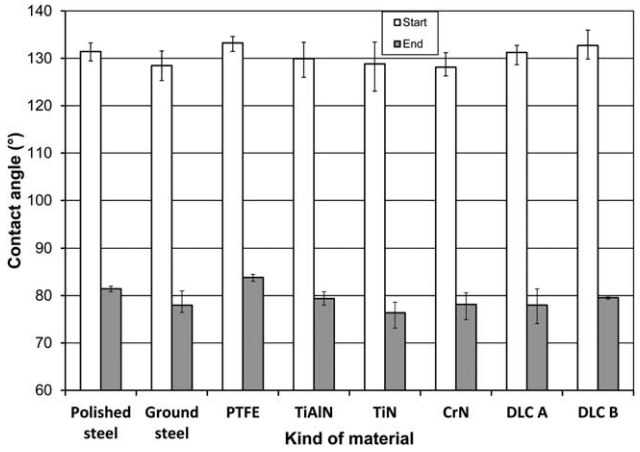

Figure 9. Contact angle of the polypropylene melt on the different surfaces at a temperature of 200 °C at the start and the end of the measuring procedure.

($\theta = 90.2°$). The contact angle is smaller on PTFE ($\theta = 101.5°$) which exhibits a low surface energy. TiN and TiAlN have the highest surface energy and lead to a lower contact angle ($\theta = 96°$). The contact angle values on ground steel and DLC A exhibit a wider range (ground steel: $\theta = 97°$, DLC A: $\theta = 99.5°$). The contact angle is 97.5° on DLC B.

There is a decrease in the contact angle of high density polyethylene with a longer measuring time. A stable contact angle is reached after approximately 600 s (on PTFE) to 900 s (on CrN) depending onthe solid surface used. The highest value of the stable contact angle is observed on PTFE ($\theta = 75.3°$) and polished steel ($\theta = 71.2°$). Ground steel and the other coatings show similar contact angle values at the end of the test runs. The contact angle values of high density polyethylene are 65.1° on ground steel, 67.4° on TiAlN, 67.8° on TiN, 66.3° on CrN, 67.7° on DLC A and 68.8° on DLC B.

Polypropylene generally has higher contact angle values compared to high density polyethylene. They are similar at the beginning of the measuring procedure and are in the range between 133.3° on PTFE and 128.5° on ground steel.

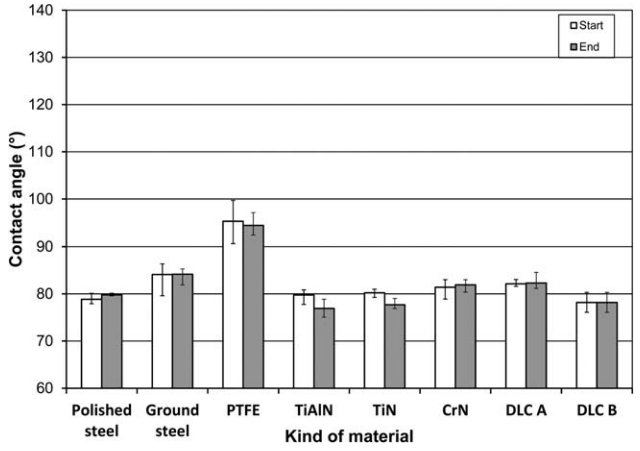

Figure 10. Contact angle of the polyamide 6.6 melt on the different surfaces at a temperature of 280 °C at the start and the end of the measuring procedure.

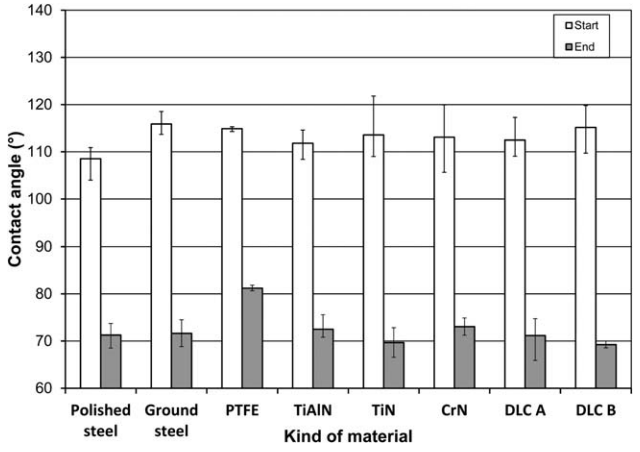

Figure 11. Contact angle of the polymethylmethacrylate melt on the different surfaces at a temperature of 250 °C at the start and the end of the measuring procedure.

There is a steeper decrease in the contact angle of polypropylene with a longer measuring time compared to high density polyethylene and no stable contact angle value can be reached. There are only small differences between the contact angle values on the different surfaces at the end of the test runs, where the contact angle is between 83.8° on PTFE and 76.4° on TiN.

Polyamide 6.6 behaves completely differently to high density polyethylene and polypropylene. First of all, the contact angle is stable from the beginning of the test (t = 0 s). Only small differences between the contact angle at the start and the end of the test procedure can be seen (Figure 10). Then, the differences in the contact angle values of polyamide 6.6 on the surfaces are larger than of the other polymeric materials investigated. At the end of the test runs the highest contact angle was determined on PTFE ($\theta = 94.4°$) and a lower value was found on ground steel ($\theta = 84.1°$). The contact angle values of polyamide 6.6 on the other solid surfaces are similar: 79.8° on polished steel, 76.9° in TiAlN, 77.7° on TiN, 81.9° on CrN, 82.3° on DLC A and 78.2° on DLC B.

Polymethylmethacrylate shows big differences in the wetting behavior dependent on time. There is a decrease in the contact angle of polymethylmethacrylate and a stable state can only be reached very late. At the beginning (t = 0 s), the contact angle values on the surfaces are similar. The wettability of the solid surfaces by polymethylmethacrylate is worse compared to high density polyethylene but better than polypropylene. The contact angle is between 115.9° on ground steel and 108.5° on polished steel.

At the end of the test runs the highest contact angle was found on PTFE ($\theta = 81.2°$). The contact angle is on the other surfaces between 69.2° on DLC B and 73° on CrN.

DISCUSSION

The obtained results show that the residence time in the high temperature chamber and the composition of the measuring atmosphere influence the wetting behavior of the polypropylene melt on the solid surfaces. With the presence of oxygen in the

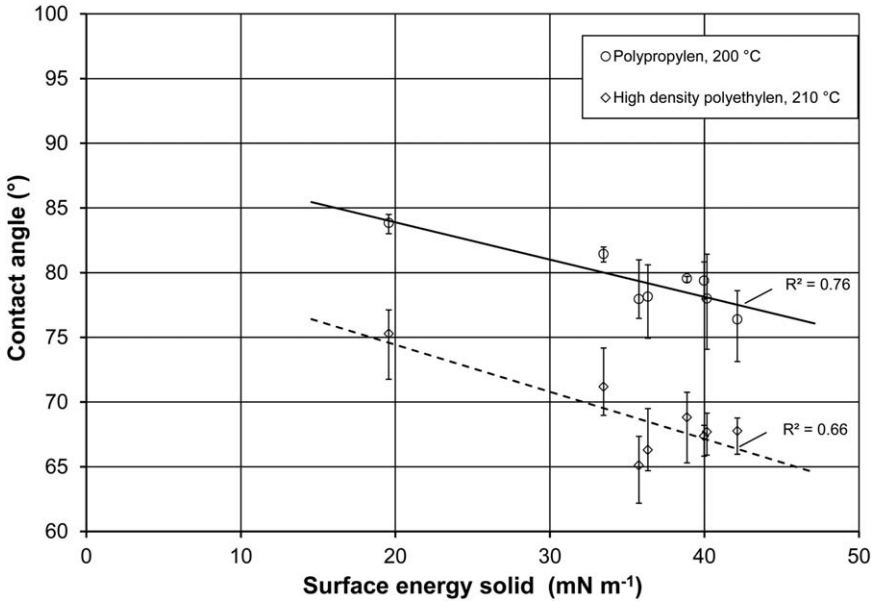

Figure 12. Contact angle of the polypropylene and the high density polyethylene melt dependent on the surface energy of the solid substrates at the end of the measuring procedure (R^2 = coefficient of determination).

measuring atmosphere a very low contact angle was observed. The oxidation of hydrocarbons such as polypropylene and polyethylene is well-known.[19] The proposed hypothesis to explain this observation is that in this experiment, oxidation takes place in the outer surface layer of the polymer melt drop. Hence, the polarity and surface tension of the polypropylene melt drop change due to its reaction with oxygen. Furthermore, this oxidation process is accompanied by a degradation of the polymer chains. The lower contact angle on the steel substrate can be related to the the change in polarity and surface tension of the outer layer of the polymer melt drop.

When using a nitrogen atmosphere, a decrease in the contact angle of polypropylene with a longer residence time can also be observed, but the final contact angle is much higher compared to air. High density polyethylene and polymethylmethacrylate also show a decrease in the contact angle with time. Polyamide 6.6 has a stable contact angle from the start.

The decrease in the contact angle of polyethylene and polymethylmethacrylate is influenced by material degradation, too. Polypropylene is more sensitive to degradation than polyethylene, because polypropylene contains tertiary carbon atoms in the main chain, where the removal of a hydrogen atom is easier than with primary or secondary carbon atoms.[19,20] Thus explaining a lower decrease in the contact angle over time and the reaching of a stable state after approx. 1200 s measuring time. Polymethylmethacrylate is also very sensitive to degradation.[21,22] Besides material degradation, the decrease in the contact angle is influenced by the time needed to reach a steady state. This result was reported by Anastasiadis, who observed a time dependent contact angle of high density polyethylene on steel and fluoropolymer coatings.[10]

The results show that a higher temperature of the polypropylene melt causes a lower contact angle on polished steel. Similar findings were also reported by Yang.[12] According to Young, the contact angle Θ depends on the surface energy of the solid σ_S, the surface tension of the liquid σ_L and the surface energy between the solid and the liquid σ_{SL}[23]

$$\cos\theta = \frac{\sigma_S - \sigma_{SL}}{\sigma_L}. \quad (7)$$

The surface tension of a liquid decreases linearly with a higher temperature according to Eötvös[24]

$$\sigma_L = \frac{0.227}{V_{mol}^{2/3}}(T_c - T), \quad (8)$$

where V_{mol} is the molar volume of the liquid, T_c is a critical temperature and T is the temperature of the liquid. Then eq. (8) is introduced in eq. (7)

$$\cos\theta = \frac{\sigma_S - \sigma_{SL}}{c_1 \cdot (T_c - T)} \quad (9)$$

and c_1 is defined as

$$c_1 = \frac{0.227}{V_{mol}^{2/3}}. \quad (10)$$

Equation (9) describes the obvious decrease in the contact angle at higher temperatures. Furthermore, changes in the surface energy of the solid can take place, which can also influence the contact angle of the polymer melt at higher temperature.

The solid substrates used have different surface properties. CrN, TiN, TiAlN, DLC A and DLC B exhibit a similar or higher surface energy and polarity than polished steel. PTFE has a much lower surface energy than polished steel and a low polarity. The measured values are in good accordance with data reported in the literature.[3,4] Correlations between the measured contact angle and the surface energy as well as the polar fraction of surface energy of the solid substrates were generated in order to obtain more information on how the difference in wettability can be explained. Figures 12 and 13 show the contact angle of the polymer melts dependent on the surface energy of the solid substrates used. The linear approximation functions of the

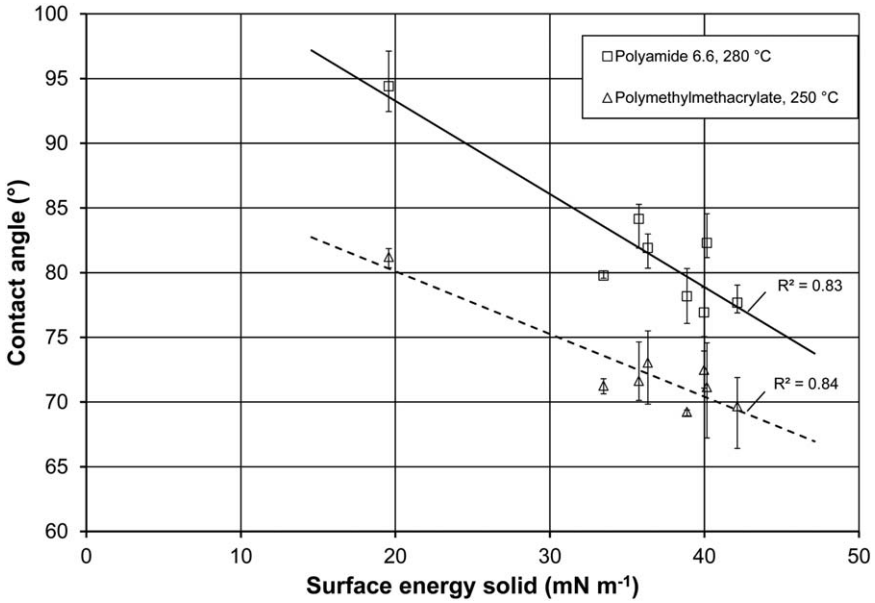

Figure 13. Contact angle of the polyamide 6.6 and the polymethylmethacrylate melt dependent on the surface energy of the solid substrate at the end of the measuring procedure (R^2 = coefficient of determination).

contact angle Θ dependent on the surface energy σ_s of the solid substrate and the values of the coefficient of determination R^2 are shown in Eq. (11) to Eq. (14).

$$\text{HDPE}: \theta = 81.7 - 0.4 \cdot \sigma_S, \quad R^2 = 0.66 \tag{11}$$

$$\text{PP}: \theta = 89.6 - 0.3 \cdot \sigma_S, \quad R^2 = 0.76 \tag{12}$$

$$\text{PMMA}: \theta = 89.8 - 0.5 \cdot \sigma_S, \quad R^2 = 0.84 \tag{13}$$

$$\text{PA 6.6}: \theta = 107.7 - 0.7 \cdot \sigma_S, \quad R^2 = 0.83 \tag{14}$$

It has to be stated that the contact angle values of the polymer melts decrease with higher surface energies of the solid surfaces. This decrease can be explained by Young's equation for the contact angle [see eq. (7)], where the surface energy of the solid is one of three parameters determining the contact angle between the liquid and the solid.[13] The slope of the linear regression lines is negative, which means that wetting of the polymer melt can be intensified by a higher surface energy of the solid.

The influence of the surface energy on the contact angle of the polymer melts investigated is of different intensity. The polymer melts can be ranked by increasing slope of the regression line as follows: polypropylene, high density polyethylene, polymethylmethacrylate and polyamide 6.6. This finding can be explained by the different surface tension of the polymer melts measured with the pendant drop method reported in literature.[11,12] Polypropylene exhibits the lowest surface tension σ_L (σ_L = 15.9 mN m^{-1} at 200 °C), followed by high density polyethylene (σ_L = 24.7 mN m^{-1} at 210 °C) and polymethylmethacrylate (σ_L = 23.6 mN m^{-1} at 250 °C). A polyamide 6 melt, which is similar to polyamide 6.6, has a surface tension of approx. 40 mN m^{-1} at 280 °C.

Figures 14 and 15 show that no clear dependence between the contact angle of the polymer melts and the polar fraction of surface energy of the solid could be found. Young's equation [see eq. (7)] considers only the total surface energy of the solid to the air, which could help explain that.[13]

Polyamide 6.6, polymethylmethacrylate and polypropylene show an increase in the contact angle with higher surface roughness of the solid steel, but high density polyethylene exhibits a decrease. The PTFE surface has the highest roughness. When including the contact angle values measured on PTFE into the considerations all polymeric materials reveal an increase in the contact angle with higher surface roughness. The higher contact angle can be attributed to a decrease in the wetted contact area between the liquid and the solid with higher roughness, as described by Cassie and Baxter for the heterogeneous wetting state [see eqs. (4) and (5), chapter Theoretical Background].[16,17] Furthermore, the results indicate that the effect of surface roughness is intensified when a solid with a low surface energy such as PTFE is used. The experiments reveal that the contact angle of the polyamide 6.6 melt is influenced more by surface roughness than the other polymeric materials. This result can be explained by the higher surface tension and higher polarity of polyamide 6.6.[11]

The difference between the contact angle values of polypropylene measured on steel surfaces with different surface roughness decreases with a longer residence time in the measuring chamber. A similar result was found for polymethylmethacrylate. Wetting of these polymeric materials is improved due to material degradation with longer residence time, which explains that the influence of surface roughness becomes much smaller. High density polyethylene and polyamide 6.6 do not show this behavior. The difference between the contact angle values measured on different rough steel surfaces remains fairly constant with longer measuring times which can be related to a better stability of these polymer melts.

Polypropylene exhibits a significant effect of temperature on the contact angle. As a prospect for future work, further experiments must be performed to investigate this temperature influence on other polymer melts and surfaces in more detail. From

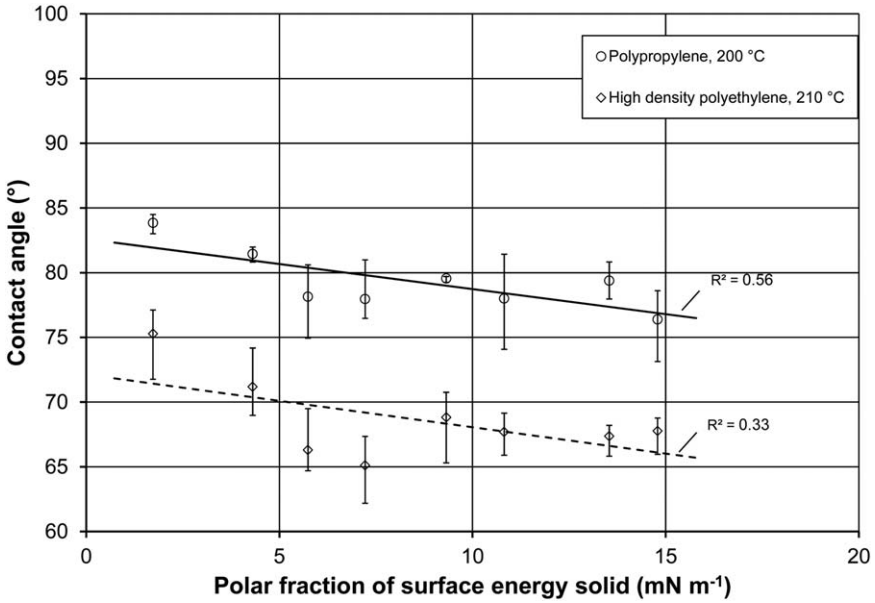

Figure 14. Contact angle of the polypropylene and the high density polyethylene melt dependent on the polar fraction of the surface energy of the solid substrates at the end of the measuring procedure (R^2 = coefficient of determination).

extrusion experience, it is well known that, when using a new screw, some running-in time is needed to achieve stable process conditions. The surface properties of the screw and tool materials and coatings can change with time while processing polymers. This so-called pre-processing influence on the contact angle must also be studied in future work.

CONCLUSIONS

In polymer processing, coatings such as TiAlN and CrN are deposited on tools, molds, and screws in order to prevent material debris and degradation, to improve the product quality as well as to reduce wear. Furthermore, wall sliding of the polymer melt and flow instabilities such as shark skin can be influenced by the tool material.

All these phenomena are related to the contact angle of the polymer melt on the solid surfaces. In this work it could be shown that at the beginning of the experiment the contact angle of melted polypropylene, high density polyethylene and polymethylmethacrylate is between 90° and 130°. At the end of the measuring runs these materials exhibit a much lower contact angle between 65° and 84°. Only polyamide 6.6 has a nearly time-independent contact angle, which is in the range between 77° and 94°.

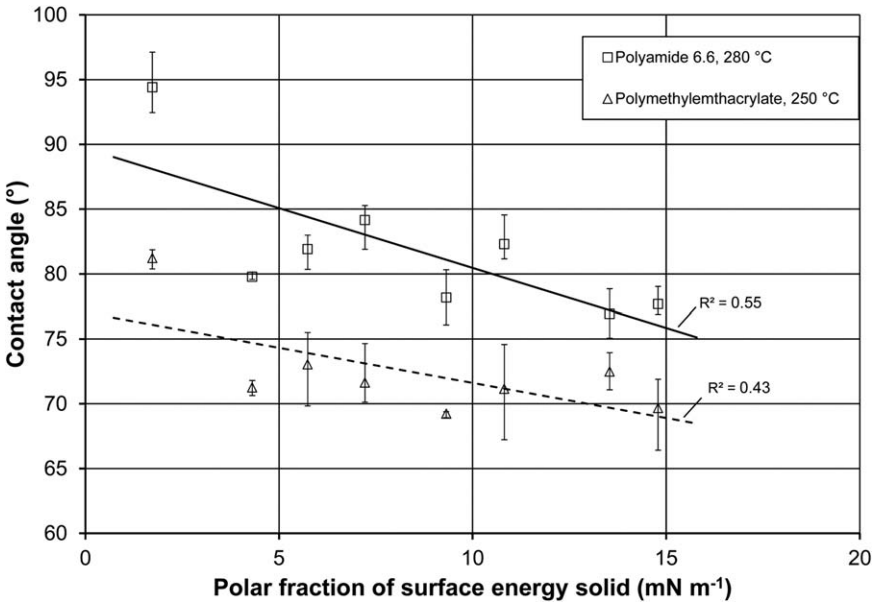

Figure 15. Contact angle of the polyamide 6.6 and the polymethylmethacrylate melt dependent on the polar fraction of the surface energy of the solid substrate at the end of the measuring procedure (R^2 = coefficient of determination).

One of the main findings of this work is that the wettability of PVD- and CVD- coatings with polymer melts is similar to steel. These coatings exhibit in general a high surface energy, which causes a rather low contact angle.

A roughening of the steel surface influences the wetting of polymer melts more than using such coating. Ideally, the solid surface should exhibit a high roughness and a low surface energy to provide a low adhesion of the polymer melt. As an example, a high contact angle was achieved on the PTFE coating due to its low surface energy and high surface roughness. The effect of roughness and the surface energy of the solid surface used on the contact angle is also dependent on the surface tension of the polymer melt. There are only slight differences in the wetting of polypropylene on the solid surfaces because of its rather low surface tension. The influence of the surface properties on the contact angle of polyamide 6.6 is more intense due to its higher surface tension.

Temperature, the residence time and the ambient atmosphere have an important influence on the measured contact angle. A better wetting of the polymer melt on the solid surfaces can be achieved at higher temperature. A longer residence time, as can occur in an extrusion tool, can cause material degradation. Material degradation is accompanied by a decrease in the contact angle of the polymer melt. The presence of oxygen causes a much lower contact angle of polypropylene on polished steel.

ACKNOWLEDGMENTS

Financial support for this work was provided by the Austrian Research Promotion Agency - FFG within the project "Plastsurf" in the framework of the funding program COIN-Aufbau.

REFERENCES

1. Worthberg, J.; Rahal, H. *J. Plast. Technol.* **2007**, *3*, 1.
2. Kayser, O. In Duisburger Extrusionstagung, March 19-20, 2013; Duisburg, Germany, **2013**.
3. Kalin, M.; Polajnar, M. *Appl. Surface Sci.* **2014**, *293*, 97.
4. Lugscheider, E.; Bobzin, K. *Surf. Coat. Technol.* **2001**, *142-144*, 755.
5. Ramamurthy, A. V. *J. Rheol.* **1986**, *25*, 55.
6. Hatzikiriakos, S. G.; Dealy, J. M. *Int. Polym. Proc.* **1993**, *9*, 36.
7. Seidel, C.; Merten, A.; Münstedt, H. *Kunststoffe Int.* **2002**, *10*, 157.
8. Zitzenbacher, G.; Bayer, T.; Huang, Z. *Int. J. Mater. Product Technol.* **2016**, *52*, 17.
9. Rauwendaal, C. In PPS 2015 (Polymer Processing Society Conference), Sept 21-25, 2015; Graz, Austria, **2015**.
10. Anastasiadis, S. H.; Hatzikiriakos, S. G. *J. Rheol.* **1998**, *42*, 795.
11. Kopczynska, A. Oberflächenspannungsphänomene bei Kunststoffen – Bestimmung und Anwendung; Ph.D. Thesis, University Erlangen-Nueremberg, July **2008**.
12. Yang, D.; Xu, Z.; Liu, C.; Wang, L. *Colloids Surf. A* **2010**, *367*, 174.
13. Young, T. *Philosoph. Trans. Roy. Soc. Lond.* **1805**, *95*, 65.
14. Wenzel, R. N. *J. Phys. Chem.* **1949**, *53*, 1466.
15. Blossey, R. *Nat. Mater.* **2003**, *2*, 301.
16. Cassie, A. B. D.; Baxter, S. *Trans. Faraday Soc.* **1944**, *40*, 546.
17. Marmur, A. *Langmuir* **2003**, *19*, 8343.
18. Owens, D. K.; Wendt, R. C. *J. Appl. Polym. Sci* **1969**, *13*, 1741.
19. Becker, R. F.; Burgin, E.; Burton, L. P. J.; Amos, S. E. In Polypropylene Handbook, 2nd ed.; Pasquini, N., Ed.; Carl Hanser Publishers: Munich, **2005**; Chapter 4, p 265.
20. Reil, M.; Kaiser, G.; Reiser, K. *Kunststoffe Int.* **2015**, *11*, 72.
21. Ferriol, M.; Gentilhomme, A.; Cochez, M.; Oget, N.; Mieloszynski, J. L. *Polym. Degrad. Stab.* **2003**, *79*, 271.
22. Wilkie, C. A. *Polym. Degrad. Stab.* **1999**, *66*, 301.
23. Pielichowski, K.; Njuguna, J. In Thermal Degradation of Polymeric Materials, 1st ed.; Smithers Rapra Publishing: England, **2005**; Chapter 5, p 41.
24. Eötvös, R. *Annalen Der Physik* **1886**, *263*, 448.